

X-RAY SPECTROSCOPY OF CANDIDATE ULTRACOMPACT X-RAY BINARIES

ADRIENNE M. JUETT¹ AND DEEPTO CHAKRABARTY

Department of Physics and Center for Space Research, Massachusetts Institute of Technology, Cambridge, MA 02139;
ajuett@virginia.edu, deepto@space.mit.edu

Accepted for publication in the Astrophysical Journal

ABSTRACT

We present high-resolution spectroscopy of the neutron star/low-mass X-ray binaries (LMXBs) 4U 1850–087 and 4U 0513–40 as part of our continuing study of known and candidate ultracompact binaries. The LMXB 4U 1850–087 is one of four systems in which we had previously inferred an unusual Ne/O ratio in the absorption along the line of sight, most likely from material local to the binaries. However, our recent *Chandra X-ray Observatory* LETGS spectrum of 4U 1850–087 finds a Ne/O ratio by number of 0.22 ± 0.05 , smaller than previously measured and consistent with the expected interstellar value. We propose that variations in the Ne/O ratio due to source variability, as previously observed in these sources, can explain the difference between the low- and high-resolution spectral results for 4U 1850–087. Our *XMM-Newton* RGS observation of 4U 0513–40 also shows no unusual abundance ratios in the absorption along the line of sight. We also present spectral results from a third candidate ultracompact binary, 4U 1822–000, whose spectrum is well fit by an absorbed power-law + blackbody model with absorption consistent with the expected interstellar value. Finally, we present the non-detection of a fourth candidate ultracompact binary, 4U 1905+000, with an upper limit on the source luminosity of $< 1 \times 10^{32}$ erg s⁻¹. Using archival data, we show that the source has entered an extended quiescent state.

Subject headings: binaries: close — stars: individual (4U 0513–40, 4U 1822–000, 4U 1850–087, 4U 1905+000) — X-rays: binaries

1. INTRODUCTION

Low-mass X-ray binaries (LMXBs) consist of a neutron star (NS) or black hole (BH) accreting material from a $\lesssim 1 M_{\odot}$ donor star. One particularly interesting subset of the LMXB population has orbital periods $\lesssim 80$ min, the predicted minimum period for binaries with hydrogen-rich main sequence donors. Such systems, commonly called ultracompact binaries, require hydrogen-deficient or degenerate companions (Joss et al. 1978; Rappaport & Joss 1984; Nelson et al. 1986). Out of the 53 LMXBs with orbital period measurements, eight systems have ultracompact periods. The growing number of known and candidate ultracompact binaries suggests that these systems make up a significant fraction of the LMXB population. We have undertaken X-ray spectral observations of one known and two candidate ultracompact binaries to better understand these unusual systems.

The LMXB 4U 1850–087 is an X-ray burster located in the globular cluster NGC 6712. It was detected by all of the major X-ray satellites since *Uhuru* and shows a roughly factor of 10 variation in flux (Forman et al. 1978; Hoffman et al. 1980; Warwick et al. 1981; Priedhorsky & Terrell 1984; Wood et al. 1984; Warwick et al. 1988; Kitamoto et al. 1992; Christian & Swank 1997; Juett et al. 2001). During the 1995 *ASCA* observation, the 0.5–10 keV X-ray flux was 3.4×10^{-10} erg cm⁻² s⁻¹ (Juett et al. 2001), which is representative of the average source flux. A low-amplitude 20.6-min periodicity, attributed to the orbital period, was reported in the *HST* data of the ultraviolet

counterpart of 4U 1850–087 (Homer et al. 1996). While this periodicity has yet to be confirmed, the X-ray to optical luminosity ratio (L_X/L_{opt}) is consistent with an ultracompact binary based on the relationship between optical magnitude, X-ray luminosity, and orbital period developed by van Paradijs & McClintock (1994). Additionally, the X-ray luminosity of 4U 1850–087 is consistent with the expected mass-transfer rate for a system with an orbital period of 21 min assuming a WD donor and gravitational radiation driven mass transfer (Homer et al. 1996).

Spectral evidence also supports an ultracompact nature for 4U 1850–087. Sidoli et al. (2001) analyzed the *BeppoSAX* spectra of the majority of the bright LMXBs located in globular clusters. They found that the best fit spectral parameters seemed to fall into two groups, with one group consisting of 4U 1820–30, 4U 1850–087, and 4U 0513–40, i.e., the known or candidate ultracompact binaries. Additionally, we found that the *ASCA* spectrum of 4U 1850–087 revealed an unusual feature at 0.7 keV also seen in three other candidate ultracompact binaries (Juett et al. 2001). We attributed this feature to an unusual Ne/O ratio in the interstellar absorption edges, presumably influenced by material local to the binary. However, a recent observation of 4U 1850–087 using *XMM-Newton* found no evidence for an unusual Ne/O ratio (Sidoli et al. 2004).

The LMXB 4U 0513–40 is an X-ray burster in the globular cluster NGC 1851. The binary was first discovered by the MIT *OSO-7* satellite and has been studied by all of the major X-ray instruments that followed (Clark et al. 1975; Johnson et al. 1977; Forman et al. 1978; McHardy et al. 1981; Hertz & Grindlay 1983; Smale & Lochner 1992; Callanan et al. 1995; Schulz

¹ Current Address: Department of Astronomy, University of Virginia, Charlottesville, VA 22903

1999; Sidoli et al. 2001). The flux from 4U 0513–40 shows a factor of ten variability from observation to observation. During the 2000 *BeppoSAX* observation, 4U 0513–40 had a 0.1–100 keV X-ray luminosity of 5×10^{36} erg s⁻¹ (Sidoli et al. 2001), an average flux for the source. Deutsch et al. (2000) identified 4U 0513–40 as a candidate ultracompact binary based on its L_X/L_{opt} ratio. In addition, its broadband optical, ultraviolet, and X-ray spectrum resembles that of other ultracompact LMXBs (Deutsch et al. 2000; Sidoli et al. 2001).

We identified the Galactic field LMXB 4U 1822–000 as an ultracompact binary candidate based on its L_X/L_{opt} ratio. The source was discovered by *Uhuru* and has been observed by all of the major X-ray missions (Giacconi et al. 1972; Markert et al. 1979; Warwick et al. 1981; Wood et al. 1984; Smale & Lochner 1992; Gottwald et al. 1995; Christian & Swank 1997). The source 4U 1822–000 has been roughly constant in flux over the course of X-ray astronomy, with a 0.5–20 keV unabsorbed flux of 1×10^{-9} erg cm⁻² s⁻¹ (Christian & Swank 1997). It has a faint optical counterpart (V=22) similar to other candidate ultracompact binaries (Chevalier & Ilovaisky 1985).

In the published literature, 4U 1905+000 was found to be persistently bright, with a 2–10 keV flux of 3×10^{-10} erg cm⁻² s⁻¹, and showed Type-I X-ray bursts (Lewin et al. 1976; Seward et al. 1976; Forman et al. 1978; Reid et al. 1980; Chevalier et al. 1985; Chevalier & Ilovaisky 1990; Gottwald et al. 1995; Christian & Swank 1997). These observations were performed in the 1970s and 1980s. The source was observed by more recent X-ray satellites, but the results of these observations have never been published. From the analysis of a radius expansion burst, Chevalier & Ilovaisky (1990) estimated the distance to 4U 1905+000 at 8 ± 1 kpc. The optical counterpart found by Chevalier & Ilovaisky (1985) is a V=20.5, ultraviolet-excess star.

In this paper, we present the results from X-ray spectral observations of 4U 1850–087, 4U 0513–40, and 4U 1822–000. The non-detection of 4U 1905+000 is also presented. The details of the observations and data reduction techniques are given in §2, and the analysis is presented in §3. In §4, we discuss the implications of these results and summarize the case for neon-rich donors in ultracompact binaries.

2. OBSERVATIONS AND DATA REDUCTION

2.1. Chandra Observation of 4U 1850–087

We observed 4U 1850–087 with the *Chandra X-ray Observatory* on 2002 August 16 for 50 ks using the Low Energy Transmission Grating Spectrometer (LETGS) and the Advanced CCD Imaging Spectrometer (ACIS; Weisskopf et al. 2002). The LETGS spectra are imaged by ACIS, an array of six CCD detectors. The LETGS/ACIS combination provides both an undispersed (zeroth order) image and dispersed spectra from the grating with a first order wavelength range of 1.4–63 Å (0.2–8.9 keV) and a spectral resolution of $\Delta\lambda = 0.05$ Å ($R = \lambda/\Delta\lambda = 28$ –1260). The various orders overlap and are sorted using the intrinsic energy resolution of the ACIS CCDs. The observation of 4U 1850–087 used a Y-offset of +1.5 in order to place the O-K absorption

edge on the back-side illuminated S3 CCD, which has suffered less degradation than the front-side illuminated CCDs. The detected zeroth and first order count rates for 4U 1850–087 were 1.2 and 3.0 cts s⁻¹, respectively.

The “level 1” event file was processed using the CIAO v3.0 data analysis package². The standard CIAO spectral reduction procedure was performed. We filtered the event file retaining those events tagged as afterglow events by the `acis_detect_afterglow` tool. Since ordering of grating spectra provides efficient rejection of background events, the afterglow detection tool is not necessary to detect cosmic ray afterglow events. No features were found that might be attributable to afterglow events. For bright sources, pileup can be a problem for CCD detectors (see e.g., Davis 2003). The zeroth order *Chandra* spectrum of 4U 1850–087 was heavily affected by pileup and was not used in this analysis. The first order spectrum suffered from minimal pileup in the 6–8 Å range (1.5–2.1 keV) which has the effect of making the instrumental iridium edge feature more pronounced. Detector response files (ARFs and RMFs) for the plus and minus first order spectra were created using the standard CIAO tools.

Calibration studies have determined that a layer of contaminant is building on the optical blocking filter of ACIS, absorbing incoming X-rays. The contaminant gradually reduces the detector quantum efficiency with time and affects all wavelengths, particularly those above 6 Å. The *Chandra* instrument teams have studied the spectral profile of the contaminant absorption using LETGS spectra and have modeled its structure and time-dependence (Marshall et al. 2004). An estimated correction for the contaminant is now available through the *Chandra* website³. The biggest effect is an overall reduction in effective area due to the large optical depth of carbon. In addition, small edges from oxygen and fluorine are also detected. The ARFs used in this analysis have been corrected for the effect of the contaminant.

The plus and minus first order spectra and response files were summed to provide a single first order spectrum and response. Background spectra were extracted from the standard LETG background regions. After background subtraction, the data were binned to a resolution of 0.075 Å to ensure good statistics. Spectral analysis of the *Chandra* observation of 4U 1850–087 was performed using ISIS (Houck & Denicola 2000).

2.2. Chandra Observation of 4U 1822–000

Chandra observed 4U 1822–000 on 2003 August 3 for 2 ks using the High Energy Transmission Grating Spectrometer (HETGS) and ACIS (Weisskopf et al. 2002). The HETGS carries two transmission gratings: the Medium Energy Gratings (MEGs) with a range of 2.5–31 Å (0.4–5.0 keV) and the High Energy Gratings (HEGs) with a range of 1.2–15 Å (0.8–10.0 keV). The HETGS spectra are imaged by ACIS, which provides both an undispersed (zeroth order) image and dispersed spectra from the gratings. The various orders overlap and are sorted using the intrinsic energy resolution of the ACIS CCDs. The first-order MEG (HEG) spectrum has a spectral resolution of $\Delta\lambda = 0.023$ Å or $R = 110$ –1350

² <http://asc.harvard.edu/ciao/>

³ See <http://asc.harvard.edu/ciao/threads/aciscontam/>

(0.012 Å or $R=100-1250$). The detected zeroth and first order count rates for 4U 1822–000 were 0.7 and 11.6 cts s^{-1} , respectively.

The level 1 event file for the 4U 1822–000 observation was processed using CIAO v3.0. The zeroth order *Chandra* spectrum of 4U 1822–000 was heavily affected by pileup (pileup fraction >80%) and was not used in this analysis. We checked the dispersed spectra of 4U 1822–000 and found that pileup was minimal (<10%). The standard CIAO tools were used to create ARFs and RMFs for the MEG and HEG +1 and –1 order spectra. The ARFs include the contamination correction mentioned previously. The ARFs were combined when the plus and minus first order spectra were added for the MEG and HEG separately. We created background spectra for the MEG and HEG using the standard background regions. The data were binned to ensure at least 50 counts per bin. The *Chandra* spectral analysis of 4U 1822–000 was performed using XSPEC v11.3 (Arnaud 1996).

2.3. XMM-Newton Observation of 4U 0513–40

The *XMM-Newton* Observatory observed 4U 0513–40 on 2003 April 1 for 24 ks. *XMM-Newton* carries three different instruments, the European Photon Imaging Cameras (EPIC; Strüder et al. 2001; Turner et al. 2001), the Reflection Grating Spectrometers (RGS; den Herder et al. 2001), and the Optical Monitor (OM; Mason et al. 2001). The OM data was not used in this analysis. The EPIC instruments consist of three CCD cameras, MOS 1, MOS 2, and pn, which provide imaging, spectral, and timing data. The pn camera was run in small window mode and the two MOS cameras were run in full window mode. The EPIC instruments provide good spectral resolution ($\Delta E=50-200$ eV FWHM) over the 0.3–12.0 keV range. There are two RGS on-board *XMM-Newton* which provide high-resolution spectra ($R=100-500$ FWHM) over the 5–38 Å (0.33–2.5 keV) range. The grating spectra are imaged onto CCD cameras similar to the EPIC-MOS cameras which allows for order sorting of the high-resolution spectra. The detected pn count rate for 4U 0513–40 was 20.8 cts s^{-1} , while the first order combined RGS count rate was 2.3 cts s^{-1} .

The *XMM-Newton* data were reduced using the Science Analysis System (SAS) version 5.4.1. Standard filters were applied to all *XMM-Newton* data. The EPIC-pn data were reduced using `epchain`. The pn spectrum was extracted from a region 45'' in radius around the source. Response files were generated for the pn spectrum using `rmfgen` and `arfgen`. We reduced the EPIC-MOS data using `emchain`. The MOS data were found to have considerable pileup and were therefore not used in this analysis. The RGS data were reduced using `rgsproc`, which produced standard first order source and background spectra and response files for both RGS. We grouped the pn spectrum to oversample the energy resolution of the CCD by no more than a factor of three. The RGS spectra were grouped to ensure that each bin had at least 20 counts. All *XMM-Newton* spectral analysis of 4U 0513–40 was performed using XSPEC (Arnaud 1996).

3. ANALYSIS AND RESULTS

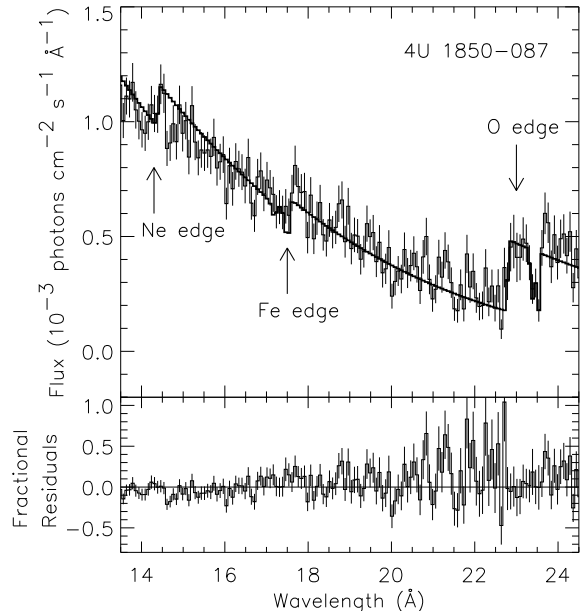


FIG. 1.— (Top panel) Combined LETG first order spectrum of 4U 1850–087 with best-fit model including the oxygen, iron, and neon edge models. (Bottom panel) Fractional residuals [(data-model)/model] of the spectral fits shown above. The absorption lines at 23.5 and 23.3 Å are the expected interstellar absorption lines from O I and O II. There are no other features detected which are consistent with narrow emission or absorption lines. The arrows mark the neon, iron, and oxygen absorption edges at 14.3, 17.5, and 23 Å respectively.

3.1. Chandra Observation of 4U 1850–087

We previously showed that 4U 1850–087 was one of four sources to have a feature at 0.7 keV in its *ASCA* spectrum which could be explained by an unusual Ne/O ratio in the absorbing material along the line of sight (Juett et al. 2001). High-resolution spectroscopy of the other three sources has confirmed the unusual Ne/O ratios (Paerels et al. 2001; Juett & Chakrabarty 2003). To investigate the absorption along the line of sight to 4U 1850–087, we fit the first order LETGS spectrum over the 1.5–25.5 Å wavelength range with a model that separately fit for the column densities of the oxygen, iron, and neon edges. The 5–10 Å wavelength range was excluded from the fits in order to avoid the piled up region of the spectrum. All errors are 90%-confidence unless otherwise noted.

The continuum model consisted of a power law + blackbody and absorption by the `tbvarabs` model with the abundances for oxygen, iron, and neon set to zero and all others equal to the interstellar abundances of Wilms et al. (2000). The equivalent hydrogen column density N_H in `tbvarabs` was set to the expected interstellar value of 2×10^{21} cm^{-2} derived from the reddening E_{B-V} to the cluster (Kuulkers et al. 2003) and using the relationship between E_{B-V} and N_H of Predehl & Schmitt (1995). The *K*-shell edges of oxygen and neon were fit using a standard `edge` model, while the Fe-*L* edge was fit using a custom multiplicative model based on the cross-sections of Kortright & Kim (2000). Two Gaussian absorption lines were included

TABLE 1
 BEST-FIT CONTINUUM SPECTRAL PARAMETERS^a

Source	Γ	A_1^b	kT_{bb} (keV)	$R_{km}^2/D_{10\text{kpc}}^2$	Flux ^c	f_{pl}^d	χ_ν^2/ν
4U 1850–087	1.48±0.05	1.32±0.09	0.479±0.009	113±13	1.45	0.66	1.3/242
4U 0513–40	1.963±0.017	2.04±0.06	0.75±0.08	2.0±0.7	0.97	0.96	1.12/1612
4U 1822–000	1.3±0.3	8±2	0.86 ^{+0.11} _{-0.07}	46 ⁺²⁶ ₋₁₇	8.4	0.73	1.47/452

^aAll errors quoted at the 90%-confidence level.

^bPower-law normalization in units of 10^{-2} photons cm^{-2} s^{-1} keV^{-1} .

^cThe absorbed 0.5–10 keV flux in units of 10^{-10} erg cm^{-2} s^{-1} .

^dFraction of the absorbed flux in the power-law component.

at the oxygen edge to represent the $1s$ - $2p$ absorption lines from O I and O II. For oxygen and neon, the atomic absorption cross-sections were taken from the theoretical calculations of Gorczyca & McLaughlin (2000) and Gorczyca (2000), respectively. The spectrum of 4U 1850–087 and best-fit spectral model including the absorption edges is shown in Figure 1. The best-fit power-law and blackbody parameters are given in Table 1. The absorbed 0.5–10 keV flux for 4U 1850–087 was 1.45×10^{-10} erg cm^{-2} s^{-1} with the power-law component contributing 66% of the flux. At a distance of 8.2 kpc (Kuulkers et al. 2003), the absorption corrected 0.5–10 keV luminosity of 4U 1850–087 was 1.35×10^{36} erg s^{-1} , assuming isotropic emission.

The best-fit absorption edge and line values are given in Table 2. The best-fit edge positions are consistent with the expected positions of the edges. We find a Ne/O ratio along the line of sight to 4U 1850–087 of 0.22 ± 0.05 , consistent with the expected interstellar value of 0.18 using the ISM abundances of Wilms et al. (2000), as well as that found in the *XMM-Newton* spectrum (Sidoli et al. 2004). The oxygen column density implies a hydrogen column density of $N_H = (4.2 \pm 0.4) \times 10^{21}$ cm^{-2} assuming standard ISM abundances (Wilms et al. 2000) in agreement with the predicted N_H from the neon and iron edges, although a factor of two larger than the expected N_H of 2×10^{21} cm^{-2} from the reddening to the cluster (Kuulkers et al. 2003). Other than the interstellar oxygen absorption lines, no other emission or absorption lines were apparent in the spectrum of 4U 1850–087. We performed a careful search of the *Chandra* spectral residuals to place limits on the presence of any spectral features in the 12–25 Å wavelength range. Gaussian models with fixed FWHM = 2000 km s^{-1} were fit at each point. (This width is similar to that seen in emission lines from other LMXBs, e.g., 4U 1626–67, Schulz et al. 2001, and EXO 0748–67, Cottam et al. 2001). From this, we can place a 3σ upper limit on the EW of any line feature, either emission or absorption (see Protassov et al. 2002, for a cautionary note). The EW limit increases with wavelength, varying from 0.05 Å at 12 Å to 0.25 Å at 24 Å.

The LETGS first order dispersed spectrum of 4U 1850–087 has an average count rate of 2.80 ± 0.17 cts s^{-1} . We examined the total count rate, as well as the count rates in two different energy ranges, to check for changes in the spectral state. We found no evidence for any change of state during the *Chandra* observation. To look for periodic modulations of the X-ray flux, we created lightcurves from event files after barycentering

and randomizing the event arrival times. (Randomizing of the event arrival times consists of adding a random quantity uniformly distributed between zero and the readout time of 0.74 s in order to avoid aliasing caused by the readout time.) We searched for modulations of the X-ray flux with frequencies between 1×10^{-5} and 5×10^{-2} Hz. We found no evidence for periodic modulation with a 90%-confidence upper limit of 1.3% for the fractional rms amplitude.

To determine the position of 4U 1850–087, we first applied the aspect offset correction available at the *Chandra* website⁴. Using the CIAO tool *celldetect*, the zeroth order source position for 4U 1850–087 was determined: R.A.=18^h53^m04^s.86 and Dec=−8°42′20″.4, equinox J2000.0 (90% confidence error radius of 0″.6). This position is 0″.6 from the optical counterpart position given by Anderson et al. (1993).

3.2. XMM-Newton Observation of 4U 0513–40

To determine the appropriate continuum model for 4U 0513–40, we fit the pn and RGS spectra simultaneously with either an absorbed power-law or an absorbed power-law + blackbody model. The pn spectrum was fit over the energy range 1.5–12 keV, while the two RGS spectra were fit over the range 0.34–2.0 keV. Residuals on the order of 10% were seen in the pn at energies between 0.5–1.5 keV. While this is consistent with estimates of the effective area calibration for the pn, given the high count rate of 4U 0513–40, these residuals resulted in inflated χ_ν^2 values so we chose to exclude this region of the pn spectrum from our fits. A constant was also included to allow for normalization differences between the pn and RGS. The absorbed power-law + blackbody model was a significantly better fit (significance of 98% as calculated by an *F*-test) to the data and we adopt this as the appropriate continuum model. The best-fit power-law and blackbody parameters are given in Table 1. The absorbed 0.5–10 keV flux for 4U 0513–40 was 9.66×10^{-11} erg cm^{-2} s^{-1} with the power-law component contributing 96% of the flux. At a distance of 12.1 kpc (Kuulkers et al. 2003), this gives a luminosity of 1.8×10^{36} erg s^{-1} .

To determine the column density along the line of sight to 4U 0513–40, we fit the RGS spectra with separate models for the absorption edges from oxygen, iron, and neon as was done for 4U 1850–087. The continuum model was fixed to that found in the pn and RGS combined fit. A Gaussian absorption line was included to

⁴ See <http://asc.harvard.edu/cal/ASPECT/celmon/index.html>

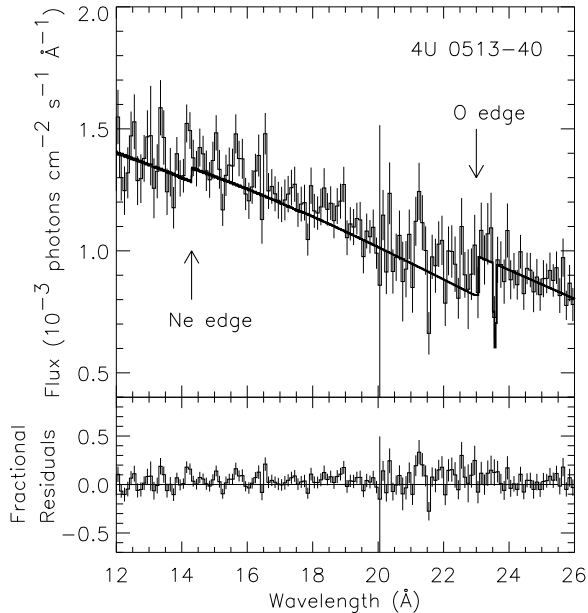


FIG. 2.— (Top panel) Combined RGS first order spectrum of 4U 0513–40 with best-fit model including the oxygen, iron, and neon edge models. (Bottom panel) Fractional residuals ($[\text{data-model}]/\text{model}$) of the spectral fits shown above. The absorption line at 23.5 Å is the expected interstellar absorption line from O I. There are no other features detected which are consistent with narrow emission or absorption lines. The arrows mark the neon and oxygen absorption edges at 14.3 and 23 Å respectively.

model the $1s-2p$ absorption line from O I. The spectrum of 4U 0513–40 and best-fit spectral model are shown in Figure 2. The best-fit absorption line and edge parameters are given in Table 2. The absorption to 4U 0513–40 is very low ($N_{\text{H}} \sim 10^{20} \text{ cm}^{-2}$) making a determination of both the wavelength and depth of the iron and neon edges difficult. We therefore fixed the iron and neon edge wavelengths to the expected values of 17.5 and 14.3 Å, respectively. Given the strength of the oxygen edge complex, its position was allowed to vary and the best-fit edge wavelength is comparable to what is found in other LMXBs (Juett et al. 2004). The oxygen edge measurement implies an equivalent hydrogen column of $N_{\text{H}} = (7.6 \pm 1.2) \times 10^{20} \text{ cm}^{-2}$ assuming standard ISM abundances (Wilms et al. 2000). The neon and iron edges are consistent with this value. The X-ray derived N_{H} value is greater than the value of $N_{\text{H}} = 1.1 \times 10^{20} \text{ cm}^{-2}$ derived from the reddening to the cluster (Kuulkers et al. 2003). No emission or absorption lines were apparent in the spectrum of 4U 0513–40. We performed a search of the *XMM-Newton* RGS spectral residuals over the 6–36 Å wavelength range. The 3σ upper limit on the EW of any spectral feature is roughly constant at 0.1 Å over the range 6–30 Å and then increases to 0.4 Å at 35 Å for Gaussian models with fixed FWHM = 2000 km s $^{-1}$ (see Protassov et al. 2002, for a cautionary note).

The 4U 0513–40 observation had average count rates of 20.8 ± 1.2 and 7.1 ± 0.6 cts s $^{-1}$ for the pn and combined RGS, respectively. Using the pn data, we checked for changes in the spectral state by examining the total

count rate, as well as the count rates in two different energy ranges. There was no evidence for a change in the spectral state of 4U 0513–40 during the *XMM-Newton* observation. Due to the low count rate of this observation ($\ll 1$ count per readout), the low frequency end of the power spectrum is affected by instrumental noise (see Kuster et al. 2002, and references therein). To remove the noise, we calculated the average power at each frequency using an 11 bin moving average and then divided by this value. We verified that the resulting powers were consistent with an exponential distribution, and then searched for modulation of the X-ray flux with frequencies between 3×10^{-4} and 1 Hz. No modulation was detected with a 90%-confidence upper limit on the fractional rms amplitude of 0.7%.

3.3. Chandra Observation of 4U 1822–000

We fit the *Chandra* HEG and MEG first-order spectra jointly with both an absorbed power-law and an absorbed power-law + blackbody model over the wavelength ranges 1.8–11.3 Å for the HEG and 2.1–14.3 Å for the MEG. The data were binned to have at least 50 counts per bin which given the low number of counts from the source resulted in significantly reduced spectral resolution. This combined with the high N_{H} along the line of sight resulted in few counts being detected shortward of 0.9 keV. Therefore, it was not necessary to use the complex absorption model presented earlier. Instead, we used the interstellar absorption model of Wilms et al. (tbabs; 2000) with the abundances in XSPEC set to *wilm* and the cross-section set to *vern*. The power-law + blackbody model produced a significantly better chi-squared value than the power-law alone (significance of 98.4% as calculated by an *F*-test), so we take a power-law + blackbody model as the appropriate continuum model for the *Chandra* spectra. The best-fit equivalent hydrogen column density was $N_{\text{H}} = (0.97 \pm 0.18) \times 10^{22} \text{ cm}^{-2}$ which compares well with the value derived from infrared dust maps ($N_{\text{H}} \approx 0.8 \times 10^{22} \text{ cm}^{-2}$; Schlegel et al. 1998). The best-fit power-law and blackbody parameters are given in Table 1. The absorbed 0.5–10 keV flux for 4U 1822–000 was $8.4 \times 10^{-10} \text{ erg cm}^{-2} \text{ s}^{-1}$ with the power-law component contributing 73% of the flux.

The combined MEG + HEG first order dispersed spectrum of 4U 1822–000 has an average count rate of 11.3 ± 0.5 cts s $^{-1}$. We examined the total count rate, as well as the count rates in two different energy ranges, to check for changes in the spectral state. We found no evidence for any change of state during the *Chandra* observation. To look for periodic modulations of the X-ray flux, we created lightcurves from event files after barycentering and randomizing the event arrival times. To increase statistics, we included events from the first through tenth grating orders. We searched for modulations of the X-ray flux with frequencies between 2×10^{-4} and 5×10^{-2} Hz. We found no evidence for periodic modulation with a 90%-confidence upper limit of 2.6% for the fractional rms amplitude.

To determine the position of 4U 1822–000, we first applied the aspect offset correction. Using the CIAO tool *tgdetect*, the zeroth order source position for 4U 1822–000 was determined: R.A. = $18^{\text{h}}25^{\text{m}}22^{\text{s}}.02$ and Dec = $-00^{\circ}00'43''.0$, equinox J2000.0 (90% confidence error radius of 0''.6). This position is 0''.9 away from the

TABLE 2
BEST-FIT ABSORPTION FEATURE PARAMETERS^a

Feature	λ (Å)	N_X (10^{18} cm ⁻²)	EW (mÅ)
4U 1850–087			
O- <i>K</i> edge	$22.79^{+0.05}_{-0.11}$	2.1 ± 0.2	...
O I 1 <i>s</i> -2 <i>p</i> line	23.511 ± 0.004	...	70 ± 30
O II 1 <i>s</i> -2 <i>p</i> line	$23.363^{+0.04}_{-0.014}$...	40 ± 40
Fe- <i>L</i> edge	17.52 ± 0.07	0.08 ± 0.03	...
Ne- <i>K</i> edge	14.40 ± 0.08	0.46 ± 0.10	...
4U 0513–40			
O- <i>K</i> edge	$23.05^{+0.13}_{-0.69}$	0.37 ± 0.06	...
O I 1 <i>s</i> -2 <i>p</i> line	$23.4^{+3.5}_{-0.9}$...	31 ± 26
Fe- <i>L</i> edge	17.5 (fixed)	< 0.014	...
Ne- <i>K</i> edge	14.3 (fixed)	0.10 ± 0.08	...

^aAll errors quoted at the 90%-confidence level.

optical counterpart position (Gottwald et al. 1991).

3.4. Chandra Observation of 4U 1905+000

We observed 4U 1905+000 on 2003 March 4 for 5 ks with *Chandra* in the HETG/ACIS configuration. We did not detect a source during this observation. From the non-detection, we place an upper limit on the flux of 1×10^{-14} erg cm⁻² s⁻¹ assuming a 0.3 keV blackbody and $N_H = 1.9 \times 10^{21}$ cm⁻². From a radius expansion burst, Chevalier & Ilovaisky (1990) derived a distance to 4U 1905+000 of 8 ± 1 kpc. At this distance, the upper limit on the source luminosity is 1×10^{32} erg s⁻¹, making 4U 1905+000 one of the faintest known quiescent NS systems.

In an effort to determine when the source went into quiescence, we retrieved the archival data from *ROSAT* and *ASCA* observations of 4U 1905+000. *ROSAT* observations of Aql X-1 would have included 4U 1905+000 in the field of view. We retrieved the two PSPCB observations of Aql X-1 performed on 1992 October 15 and 1993 March 24. No source at the position of 4U 1905+000 was found with an upper limit on the flux of 6×10^{-13} erg cm⁻² s⁻¹. Similarly, the *ASCA* observation of 4U 1905+000 performed on 1995 April 09 found no source at the position of 4U 1905+000. From this work, we conclude that 4U 1905+000 went into its quiescent state in the late 1980s or early 1990s after an extended outburst phase.

4. DISCUSSION

In this paper, we have shown that the *Chandra*/LETGS spectrum of 4U 1850–087, the *XMM-Newton*/RGS spectrum of 4U 0513–40, and the *Chandra*/HETGS spectrum of 4U 1822–000 are all well fit by an absorbed power-law + blackbody model. No unusual abundance ratios are implied by the detected absorption features, and no emission or absorption features were found other than the expected absorption lines due to interstellar oxygen. For 4U 1850–087, this is significantly different from what is implied by the earlier *ASCA* observation, which had established 4U 1850–087 as being part of a class of four NS/LMXBs all having a similar feature at 0.7 keV in their low-resolution spectra (Juett et al. 2001). This feature had originally been attributed to unresolved line emission from iron and oxygen (see e.g., Christian et al. 1994; White et al. 1997).

However, a high-resolution observation of the brightest of these sources, 4U 0614+091, with *Chandra*, failed to detect any emission lines, finding instead an unusually high Ne/O number ratio in the absorption along the line of sight (Paerels et al. 2001). We had subsequently pointed out that the *ASCA* spectra of all four sources are well fit without a 0.7 keV emission line using a model that includes photoelectric absorption due to excess neon along the lines of sight and presumably local to the sources (Juett et al. 2001).

Of the other four sources that we previously proposed as neon-rich systems based on their low-resolution *ASCA* spectra, three (4U 0614+091, 2S 0918–549, and 4U 1543–624) have also shown unusual Ne/O abundance ratios in their high-resolution X-ray spectra (Paerels et al. 2001; Juett & Chakrabarty 2003). However, a comparison of the *Chandra*, *XMM-Newton*, and *ASCA* results for 2S 0918–549 and 4U 1543–624 also revealed variability in the measured Ne/O ratio, which seemed to be associated with changes in the source continuum properties (Juett & Chakrabarty 2003). We previously suggested that changes in the spectral properties of the sources could lead to ionization effects that would produce the variable Ne/O ratio found for the neutral edges. Ionization would affect oxygen more than neon, inflating the measured neutral Ne/O ratio. Unfortunately, this means that the measured Ne/O ratio would not reflect the donor composition.

Here we propose that for 4U 1850–087 as well, ionization effects due to continuum spectral variations are also responsible for the differences between the *ASCA* and *Chandra* results. When the *Chandra* spectrum is rebinned to a resolution comparable to that of *ASCA*, the *Chandra* data do not show the 0.7 keV feature seen previously with *ASCA* (see Figure 3). This clearly indicates that the source spectrum changed between 1995 and 2002. Given our interpretation of the feature as being due to an unusual Ne/O ratio in the absorbing material, the lack of the 0.7 keV feature in the *Chandra* spectrum is consistent with the measured Ne/O ratio of 0.22 ± 0.05 , which is close to the interstellar value. Had the feature still been present in the binned *Chandra* spectrum, then our interpretation would have been incorrect. The variation of the Ne/O ratio in the absorbing material is accompanied by differences in the continuum spectral

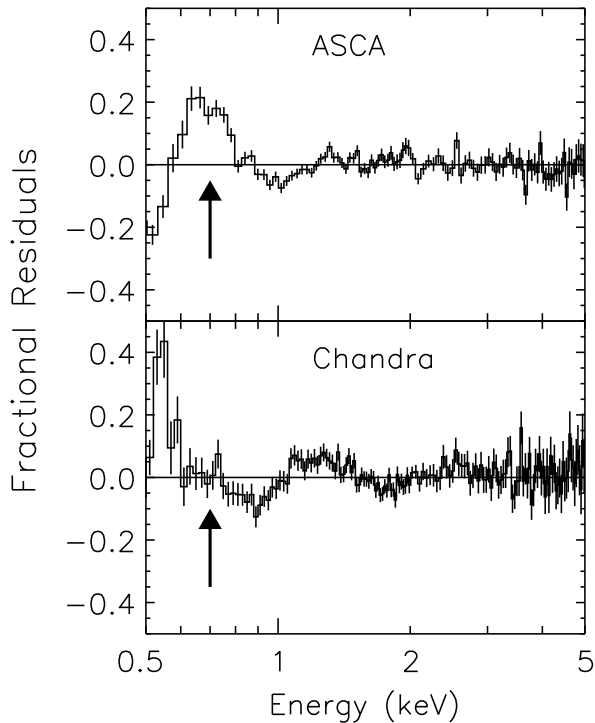


FIG. 3.— Comparison of the *ASCA* (top panel) and *Chandra* (bottom panel) spectrum for 4U 1850–087 plotted at the same energy resolution. Shown are the fractional residuals ($[\text{data} - \text{model}]/\text{model}$) of an absorbed power law + blackbody model. The *ASCA* spectrum shows a residual feature at 0.7 keV (marked by an arrow) which is absent in the *Chandra* data. This feature was previously attributed to an unusual Ne/O abundance ratio in the absorption. The lack of the 0.7 keV feature in the *Chandra* spectrum supports our suggestion that the source spectrum has changed between the two observations. The residual in the *Chandra* spectrum at 0.55 keV is due to misalignment of the oxygen edge between the data and model.

properties of 4U 1850–087. The *Chandra* observation of 4U 1850–087 was taken during a lower luminosity state than the *ASCA* observation which showed the unusual Ne/O ratio. This is comparable to what was observed in the other proposed neon-rich sources 2S 0918–549 and 4U 1543–624. A more detailed analysis of the *XMM-Newton* data may shed more light on this source. Given

that the *XMM-Newton* results show a Ne/O ratio similar to that found in the *Chandra* data (Sidoli et al. 2004), we would expect that the continuum properties should also be similar.

While X-ray spectra may be inconclusive in determining the donor composition of these systems, new results from optical spectroscopy have confirmed their unusual nature. Optical spectra of three candidate ultracompact binaries with suggested neon-rich donors, 4U 0614+091, 4U 1543–624, and 2S 0918–549 (Juett et al. 2001), showed no prominent hydrogen or helium emission lines (Nelemans et al. 2004; Wang 2004). In the brightest of these, 4U 0614+091, Nelemans et al. (2004) found emission lines which they attributed to carbon and oxygen. The other spectra were not as high quality, but hints of similar spectral features were seen. The optical spectra seem to confirm our suggestion that the donors in these systems are C-O WDs (Juett et al. 2001; Nelemans et al. 2004). The notion of a class of ultracompact LMXBs with neon-rich C-O WD donors is motivated by the definite detection of one such system, 4U 1626–67 (Schulz et al. 2001; Homer et al. 2002). However, not all ultracompact binaries are expected to have C-O donors. The burst properties of the 11-min binary 4U 1820–30 support a helium WD donor for that system, while the properties of the 50-min X-ray dipper 4U 1916–05 point to a hydrogen-deficient but not yet degenerate donor. As more observations allow for the donor compositions of the ultracompact binaries to be determined, the results will provide a unique test of binary evolution theory. Multiwavelength observations may be the best way of determining the donor properties in ultracompact binary systems.

Partial support for this work was provided by NASA through *Chandra* award numbers GO2-3065X and GO3-4055X issued by the *Chandra* X-Ray Observatory Center, which is operated by the Smithsonian Astrophysical Observatory for NASA under contract NAS8-03060. This work was also supported in part by NASA under grants NAG5-13179 and NAG5-9184 as well as contract NAS8-01129. This research made use of data obtained through the High Energy Astrophysics Science Archive Research Center (HEASARC), operated by the NASA/Goddard Space Flight Center.

REFERENCES

- Anderson, S. F., Margon, B., Deutsch, E. W., & Downes, R. A. 1993, *AJ*, 106, 1049
- Arnaud, K. A. 1996, in *ASP Conf. Ser. 101: Astronomical Data Analysis Software and Systems V*, 17
- Callanan, P. J., Penny, A. J., & Charles, P. A. 1995, *MNRAS*, 273, 201
- Chevalier, C., & Ilovaisky, S. A. 1985, *Space Science Reviews*, 40, 443
- . 1990, *A&A*, 228, 115
- Chevalier, C., Ilovaisky, S. A., & Charles, P. A. 1985, *A&A*, 147, L3
- Christian, D. J., & Swank, J. H. 1997, *ApJS*, 109, 177
- Christian, D. J., White, N. E., & Swank, J. H. 1994, *ApJ*, 422, 791
- Clark, G. W., Markert, T. H., & Li, F. K. 1975, *ApJ*, 199, L93
- Cottam, J., Kahn, S. M., Brinkman, A. C., den Herder, J. W., & Erd, C. 2001, *A&A*, 365, L277
- Davis, J. E. 2003, in *Proceedings of the SPIE, Vol. 4851, X-Ray and Gamma-Ray Telescopes and Instruments for Astronomy*, ed. J. E. Truemper & H. D. Tananbaum, 101
- den Herder, J. W., et al. 2001, *A&A*, 365, L7
- Deutsch, E. W., Margon, B., & Anderson, S. F. 2000, *ApJ*, 530, L21
- Forman, W., Jones, C., Cominsky, L., Julien, P., Murray, S., Peters, G., Tananbaum, H., & Giacconi, R. 1978, *ApJS*, 38, 357
- Giacconi, R., Murray, S., Gursky, H., Kellogg, E., Schreier, E., & Tananbaum, H. 1972, *ApJ*, 178, 281
- Gorczyca, T. W. 2000, *Phys. Rev. A*, 61, 024702
- Gorczyca, T. W., & McLaughlin, B. M. 2000, *Journal of Physics B Atomic Molecular Physics*, 33, L859
- Gottwald, M., Parmar, A. N., Reynolds, A. P., White, N. E., Peacock, A., & Taylor, B. G. 1995, *A&AS*, 109, 9
- Gottwald, M., Steinle, H., Pietsch, W., & Graser, U. 1991, *A&AS*, 89, 367
- Hertz, P., & Grindlay, J. E. 1983, *ApJ*, 275, 105

- Hoffman, J. A., Cominsky, L., & Lewin, W. H. G. 1980, *ApJ*, 240, L27
- Homer, L., Anderson, S. F., Wachter, S., & Margon, B. 2002, *AJ*, 124, 3348
- Homer, L., Charles, P. A., Naylor, T., van Paradijs, J., Auriere, M., & Koch-Miramond, L. 1996, *MNRAS*, 282, L37
- Houck, J. C., & Denicola, L. A. 2000, in *ASP Conf. Ser.* 216: *Astronomical Data Analysis Software and Systems IX*, Vol. 9, 591
- Johnson, H. M., Catura, R. C., Charles, P. A., & Sanford, P. W. 1977, *ApJ*, 212, 112
- Joss, P. C., Avni, Y., & Rappaport, S. 1978, *ApJ*, 221, 645
- Juett, A. M., & Chakrabarty, D. 2003, *ApJ*, 599, 498
- Juett, A. M., Psaltis, D., & Chakrabarty, D. 2001, *ApJ*, 560, L59
- Juett, A. M., Schulz, N. S., & Chakrabarty, D. 2004, *ApJ*, 612, 308
- Kitamoto, S., Tsunemi, H., & Roussel-Dupre, D. 1992, *ApJ*, 391, 220
- Kortright, J. B., & Kim, S. 2000, *Phys. Rev. B*, 62, 12216
- Kuster, M., Kendziorra, E., Benlloch, S., Becker, W., Lammers, U., Vacanti, G., & Serpell, E. 2002, in *New Visions of the X-ray Universe in the XMM-Newton and Chandra Era*, (astro-ph/0203207)
- Kuulkers, E., den Hartog, P. R., in't Zand, J. J. M., Verbunt, F. W. M., Harris, W. E., & Cocchi, M. 2003, *A&A*, 399, 663
- Lewin, W. H. G., Li, F. K., Hoffman, J. A., Doty, J., Buff, J., Clark, G. W., & Rappaport, S. 1976, *MNRAS*, 177, 93P
- Markert, T. H., et al. 1979, *ApJS*, 39, 573
- Marshall, H. L., Tennant, A., Grant, C. E., Hitchcock, A. P., O'Dell, S., & Plucinsky, P. P. 2004, in *Proceedings of the SPIE*, Vol. 5165, *X-Ray and Gamma-Ray Instrumentation for Astronomy*, ed. K. A. Flanagan & O. H. Siegmund, 497
- Mason, K. O., et al. 2001, *A&A*, 365, L36
- McHardy, I. M., Lawrence, A., Pye, J. P., & Pounds, K. A. 1981, *MNRAS*, 197, 893
- Nelemans, G., Jonker, P. G., Marsh, T. R., & van der Klis, M. 2004, *MNRAS*, 348, L7
- Nelson, L. A., Rappaport, S. A., & Joss, P. C. 1986, *ApJ*, 304, 231
- Paerels, F., et al. 2001, *ApJ*, 546, 338
- Predehl, P., & Schmitt, J. H. M. M. 1995, *A&A*, 293, 889
- Priedhorsky, W. C., & Terrell, J. 1984, *ApJ*, 280, 661
- Protassov, R., van Dyk, D. A., Connors, A., Kashyap, V. L., & Siemiginowska, A. 2002, *ApJ*, 571, 545
- Rappaport, S., & Joss, P. C. 1984, *ApJ*, 283, 232
- Reid, C. A., Johnston, M. D., Bradt, H. V., Doxsey, R. E., Griffiths, R. E., & Schwartz, D. A. 1980, *AJ*, 85, 1062
- Schlegel, D. J., Finkbeiner, D. P., & Davis, M. 1998, *ApJ*, 500, 525
- Schulz, N. S. 1999, *ApJ*, 511, 304
- Schulz, N. S., Chakrabarty, D., Marshall, H. L., Canizares, C. R., Lee, J. C., & Houck, J. 2001, *ApJ*, 563, 941
- Seward, F. D., Page, C. G., Turner, M. J. L., & Pounds, K. A. 1976, *MNRAS*, 175, 39P
- Sidoli, L., Parmar, A. N., & Oosterbroek, T. 2004, in *The INTEGRAL Universe*, to be published, (astro-ph/0404039)
- Sidoli, L., Parmar, A. N., Oosterbroek, T., Stella, L., Verbunt, F., Masetti, N., & Dal Fiume, D. 2001, *A&A*, 368, 451
- Smale, A. P., & Lochner, J. C. 1992, *ApJ*, 395, 582
- Strüder, L., et al. 2001, *A&A*, 365, L18
- Turner, M. J. L., et al. 2001, *A&A*, 365, L27
- van Paradijs, J., & McClintock, J. E. 1994, *A&A*, 290, 133
- Wang, Z. 2004, PhD thesis, Massachusetts Institute of Technology
- Warwick, R. S., et al. 1981, *MNRAS*, 197, 865
- Warwick, R. S., Norton, A. J., Turner, M. J. L., Watson, M. G., & Willingale, R. 1988, *MNRAS*, 232, 551
- Weisskopf, M. C., Brinkman, B., Canizares, C., Garmire, G., Murray, S., & Van Speybroeck, L. P. 2002, *PASP*, 114, 1
- White, N. E., Kallman, T. R., & Angelini, L. 1997, in *X-Ray Imaging and Spectroscopy of Cosmic Hot Plasmas*, ed. F. Makino & K. Mitsuda (Universal Academy Press), 411
- Wilms, J., Allen, A., & McCray, R. 2000, *ApJ*, 542, 914
- Wood, K. S., et al. 1984, *ApJS*, 56, 507